Article

Simply Constructed and Highly Efficient Classified Cargo-discharge DNA Robot: A Novel DNA Walking Nanomachine Platform for Ultrasensitive Multiplexed Sensing

Yuanyuan Chang, Zhongyu Wu, Qianxin Sun, Ying Zhuo, Yaqin Chai, and Ruo Yuan

Anal. Chem., **Just Accepted Manuscript** • DOI: 10.1021/acs.analchem.9b00363 • Publication Date (Web): 07 Jun 2019

Simply Constructed and Highly Efficient Classified Cargo-discharge DNA Robot: A Novel DNA Walking Nanomachine Platform for Ultrasensitive Multiplexed Sensing

Yuanyuan Chang, Zhongyu Wu, Qianxin Sun, Ying Zhuo, Yaqin Chai,* Ruo Yuan*

Key Laboratory of Luminescent and Real-Time Analytical Chemistry (Southwest University), Ministry of Education, College of Chemistry and Chemical Engineering, Southwest University, Chongqing 400715, PR China

* Corresponding author. Tel.: +86-23-68252277; Fax: +86-23-68253172.

E-mail address: yqchai@swu.edu.cn ; yuanruo@swu.edu.cn

*Corresponding authors at: Tel.: +86-23-68252277, fax: +86-23-68253172.
E-mail addresses: yqchai@swu.edu.cn (Y. Q. Chai); yuanruo@swu.edu.cn (R. Yuan).

ABSTRACT

In this work, a classified cargo-discharge DNA robot with only two DNA strands was designed and driven by analogous proximity ligation assay (aPLA)-based enzyme cleaving for fast walk to construct a novel electrochemical biosensor for simultaneously ultrasensitive detection of microRNA-155 (miRNA-155) and miRNA-21. Compared with traditional DNA nanomachines, the multifunctional DNA robot possessed simple structure, high self-assembling efficiency and walking efficiency. Once it interacted with target miRNAs, this DNA robot could fast walk on the electrode surface and realize the classified cargoes discharging including beacons methylene blue (MB) and ferrocene (Fc) respectively labeled in the double stranded DNA (A1-A2) for ultrasensitive detection of multiple miRNAs simultaneously. As a result, the wide linearity ranging from 100 aM to 100 pM and low detection limit of 42.7 aM and 51.1 aM were obtained for miRNA-155 and miRNA-21 detection respectively. As a proof of concept, the present strategy initiates a novel and high efficient walking platform to realize the ultrasensitive detection of biomarkers and possesses the potential applications in clinical diagnosis of disease.

KEYWORDS: DNA robot, proximity ligation assay, enzyme cleaving, microRNA detection, electrochemical biosensor

INTRODUCTION

Molecular machines that carry out mechanical tasks are key functional components in all biological organisms,[1-4] therefore, various artificial molecular machines are designed to study their action mechanisms in biological organisms, for example, DNA

motor,[5,6] motor proteins,[7,8] molecular muscle,[9] and so on. DNA as a critical biomolecule in genetics and biology possesses double-helical structure and the Watson-Crick pairing of its bases to enable DNA structurally predictable,[10-12] which makes it to be possible for the design and synthesis of artificial DNA nanostructures by suitable programming of the base sequences of DNA strands.[13-16] Therefore, a variety of DNA nanomachines have been designed and assembled for different applications, such as, DNA walker,[17,18] DNA robot,[19,20] DNA tweezers, [21,22] DNA roller,[23] etc. Although these molecular machines could carry out complex nanomechanical tasks automatically, most of them were designed to perform a single function: walking in a controlled direction, while few demonstrations involved a second function combined with walking (such as, discharging or picking up nanoparticles) owing that relatively more complex functions were more difficult to control, as well as limited to what the DNA nanomachines can perform only a few steps.[19] Moreover, multifunctional nanomachines also demand large amounts of DNA strands and complex design, leading to the increasing experiment cost and time-consuming. Thus, how to avoid the above predicaments for the design of programmable DNA nanomachines that spontaneously execute multifunctional nanomechanical tasks is still a challenge.

The walking of DNA nanomachines is usually driven by several common types in previous researches, for instances, light,[24,25] strand displacement,[18,26] enzyme. [27,28]Although the light could achieve the fast walking for DNA nanomachines, the driven usually demands with the help of chemical and electrical inputs, then it will

become common to perform, which compels it to be at the development stage.[29] Moreover, the walking of DNA nanomachines driven by strand displacement is usually aided by the exponentially increasing cost of oligonucleotide preparation and purification, accompanying larger numbers of DNA strands waste,[30] therefore, enzyme as high efficient method has become the best candidate for driving the walking of DNA nanomachines in recent years.[5,31,32] However, the traditional enzyme driven is usually suffered with complex design of DNA sequence for stabilizing the structure in addition to the design of multiple enzyme shear sites in some biosensors for multiple detection, which requires high cost and fussy experimental operation. Hence, it has become a burning issue by combining with some other methods to realize the fast and high efficient enzyme driven for the walking of DNA nanomachines. The proximity ligation assay (PLA) could prevent spatial diffusion by the strong binding of two affinity ligands to target proteins, thus complementary-oligonucleotide proximity could be closed and then dramatically increase their local effective concentrations, further enhanced the efficiency and stability of the hybrid, and accelerated the reaction rate.[33,34] Inspired by this mechanism, the analogous PLA (aPLA) induced by DNA has aroused widespread concern attributing that it entirely inherits the inherent advantages of PLA, as well as can obtain more stable DNA structure with only several bases, simplifying sequence design and intensifying operational flexibility,[35,36] but, the study involving aPLA-based enzyme cleaving for driving the walking of DNA nanomachines has not

been reported, which provides a precious opportunity to pave an avenue for driving the walking of DNA nanostructured robot with more simple and faster way.

Hence, a simply constructed and highly efficient classified cargo-discharge DNA robot was well-designed with only two DNA strands and driven by aPLA-based enzyme cleaving to fast walk around on the electrode surface to construct an electrochemical biosensor for ultrasensitive the detection of multiple miRNAs. As shown in the Scheme 1, the construction of the proposed electrochemical biosensor is as follows: first, the GCE was modified with dep-Au, then the formed double strand DNA (A1-A2) labeled with MB and Fc respectively was captured on the electrode surface via Au-N bonding and then blocked with HT. When the designed DNA robot, target miRNA-21, miRNA-155 and Nt.BbvCI were introduced into this system simultaneously, the electrochemical signals decreased significantly owing that the targets could close the two feet of DNA robot to trigger PLA-based enzyme cleaving for classified release of DNA fragments labeled with MB or Fc, realizing the multiple targets detection. In a word, the functions of the designed DNA robot as follows: (1) capture two different targets, (2) walk on the electrode surface, (3) classifiedly discharge the DNA fragments labeled with MB and Fc. By this design, the electrochemical biosensor could initiate a novel and high efficient walking platform to realize the highly sensitive detection of multiple miRNAs or other biomarkers.

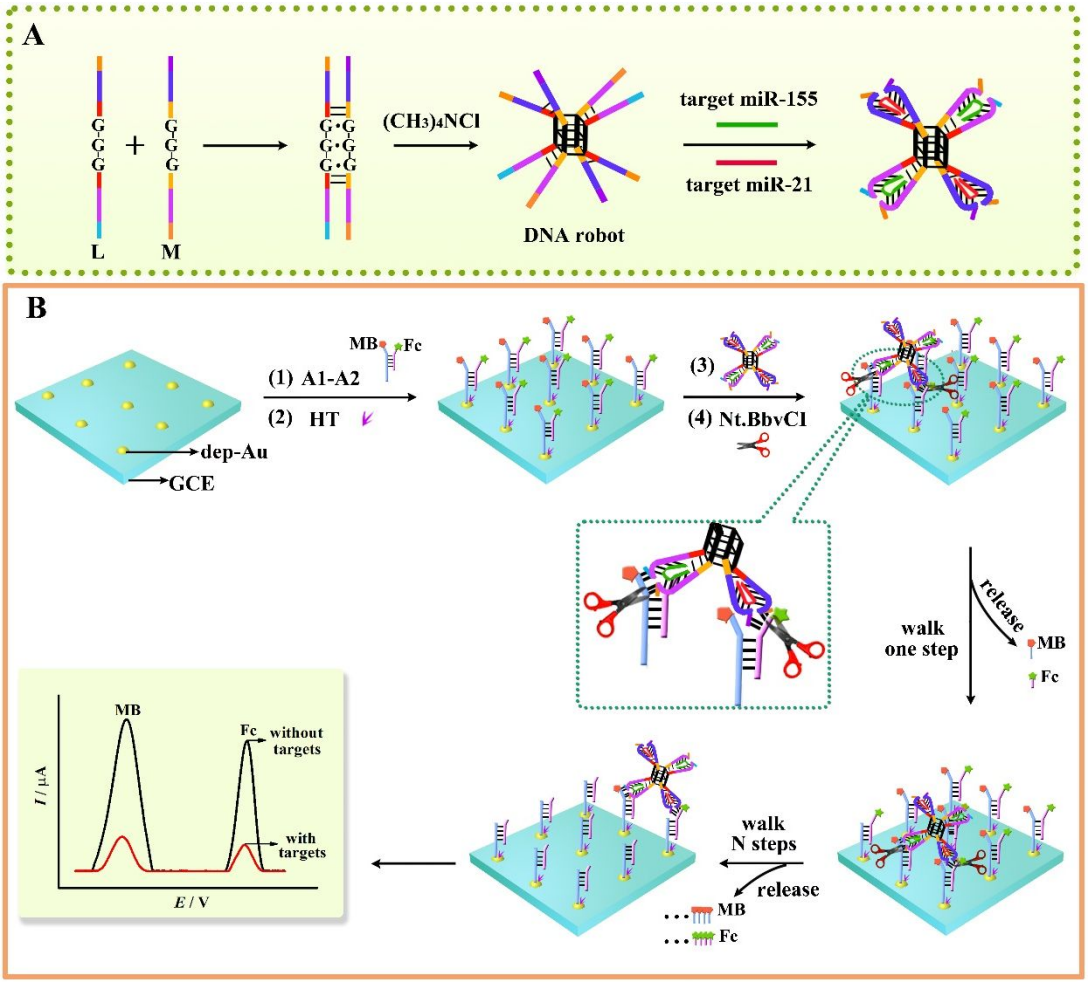

Scheme 1 Schematic illustrations of (A) the formation of classified cargo-discharge DNA robot, (B) the detection principle of the electrochemical biosensor for multiple miRNAs detection based on classified cargo-discharge DNA robot.

EXPERIMENTAL SECTION

Chemicals and Materials. Chloroauric acid ($HAuCl_4$) and mercaptoethanol (HT) were purchased from Sigma (St. Louis, MO, USA). Alumina polishing powder was obtained from Tianjin Aida Hengsheng Technology Development Co. Ltd (Tianjin, China). Nt.BbvCI enzyme, HPLC-purified, synthetic microRNAs (miRNA) and all other oligonucleotides were obtained from Shanghai Sangon Biological Engineering Technology & Services Co., Ltd (Shanghai, China). All nucleotides sequences were

listed in the Table 1. Aqueous solutions were prepared using ultrapure water (specific resistance of 18 MΩ·cm). Other reagents were of analytical grade and used as received.

Table 1 The oligonucleotide sequences applied in the proposed work

oligonucleotide	Sequence (5′ to 3′)
A1	TGATTCAATCCTCTTGCGCATCTATAAATTTTTTTCATTCGGCTGAGG-MB
A2	Fc-GCTGAGGACTAAGTTTTTTATTTATAGATGCGCAAGAGGATTGAATCA-NH_2
L	CCTCAGCCTGATAAGCTATTTCTCGAGAAGCTCCTGATTGGGTGGGTTTGTGGTTCAAGGATCCTTTACCCCTATCACCCTCAGC
M	ACTTAGTGATTAGCATTAATTTGGATCCTTGAACCACATTGGGTGGGTTTCAGGAGCTTCTCGAGTTTTCAACATCAGTCGAATGA
miRNA-155	UUAAUGCUAAUCGUGAUAGGGGU
miRNA-21	UAGCUUAUCAGACUGAUGUUGA
miRNA-141	UAACACUGUCUGGUAAAGAUGG
miRNA-let-7a	UGAGGUAGUAGGUUGUAUAGUU
miRNA-182-5p	UUU GGC AAU GGU AGA ACU CAC ACU

Apparatus. All electrochemical measurements were performed in a conventional electrochemical cell including a recorded with CHI 760E electrochemical workstation (Shanghai Chenhua Instrument, China) and three-electrode arrangement. Square wave voltammetry (SWV) in this work was performed in 2 mL PBS with the potential range from -0.6 to 0.7 V at 100 mV/s. The morphology of nanomaterials was characterized via a scanning electron microscope (SEM, S-4800, Hitachi, Japan) with an acceleration voltage of 20-30 kV. Ultrapure water was acquired from a Nanopure

Infinity ultrapure water system (Barnstead thermolyne Corporation, Dubuque, IA, USA). All Data was handled with “linear baseline correction” function and “smooth” function of CHI760E software.

Preparation of DNA robot. The synthetic L (2 μM) and M (2 μM) DNA strands were mixed together in tetramethylammonium chloride (TMACl) buffer (1.0 mM TMACl; 10 mM Tris, pH 7.9), then heated to 95 °C for 2 min, and allowed to cool to 37 °C slowly, then reacted for 15 min.

The Fabrication of the Modified Electrodes. Firstly, the cleaned bare GCE was electrodeposited for 30s in the $HAuCl_4$ (1％) solution (1％ stands for the mass ratio of solute ($HAuCl_4$) and solution during the solvent is H_2O) for the formation of dep-Au, then the double strand DNA (A1-A2) was introduced into this biosensor by Au-N bonding for 16 h. In order to block the non-specific sites on the modified electrode surface, 20 μL HT was immobilized for 50 min. Subsequently, the mixture of the formed DNA robot (8 μL), the target of miRNA-21 (5 μL) and miRNA-155 (5 μL), and Nt.BbvCI (2 μL, 2U/μL) were introduced into this modified electrode surface with 40 min. Finally, all experimental steps were respectively cleaned by ultrapure water, and the as-prepared electrode was further dealt with electrochemical measurements.

RESULTS AND DISCUSSIONS

Optimization of the Experimental Conditions. The successful formation of DNA robot is the key factor for this prepared electrochemical biosensor, thus the concentration of tetramethylammonium chloride (TMACl) for the formation of DNA

robot, the incubation time of forming DNA robot and target were investigated respectively. Firstly, different concentrations of TMACl including 0.5 mM, 1.0 mM, 1.5 mM, 2.0 mM, 2.5 mM and 3.0 mM were used for optimizing the best concentration of TMACl for the formation of DNA robot by polyacrylamide gel electrophoresis (PAGE). From Figure 1A, the band of DNA corresponding to the 0.5 mM TMACl was at the low position. Once the concentration of TMACl increased to 1.0 mM, the band of DNA reached at high position and remained unchanged until 3.0 mM, demonstrating that the DNA robot was formed at 1.0 mM TMACl. thus, 1.0 mM was selected as the best the concentration of TMACl for the formation of DNA robot. Moreover, the immobilization time of forming DNA robot was also surveyed with PAGE, and the results were presented in the Figure 1B. As we can see from Figure 1B, as the increasing time, the positions of these DNA bands rose gradually and kept unchanged until 15 min, thus 15 min was as the best immobilization time for forming DNA robot. Finally, the incubation time for targets was examined by changing different time of 10 min, 20 min, 30 min, 40 min, 50 min, 60 min. From Figure 1C, with the time increasing, the current response of MB and Fc simultaneously decreased and arrived a platform at 40 min. Thus, in order to obtain optimum results for miRNA-155 and miRNA-21 detection, 40 min was served as the optimal incubation time of targets.

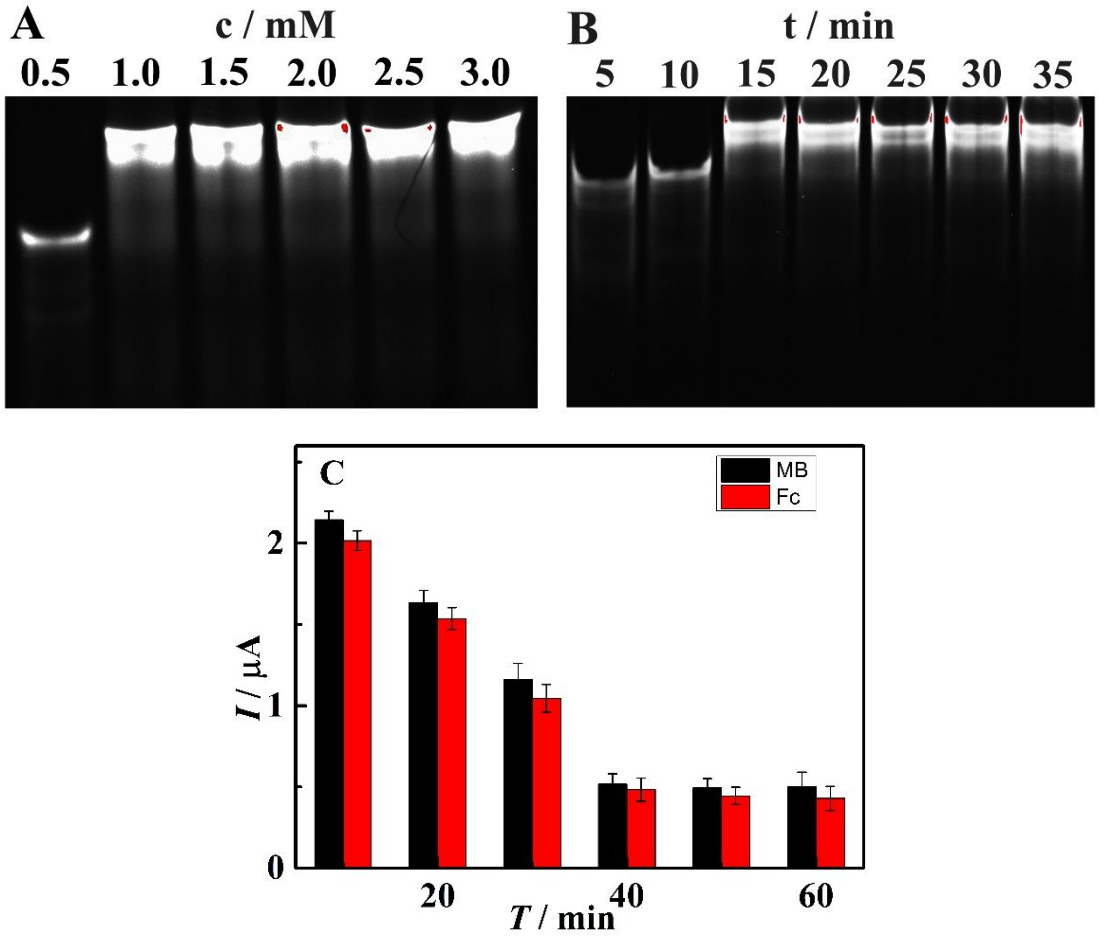

Figure 1. (A) Optimum reaction concentration of tetramethylammonium chloride (TMACl), the time for the formation of DNA robot (B) and the reaction time of targets (C).

Stepwise Characterization of the Modified Electrode. The successful fabrication of this biosensor for miRNA-155 and miRNA-21 detection was recorded with CV and SWV measurements in 2 mL $[Fe(CN)_6]^{3-/4-}$ (5mM, pH 7.4) and PBS solution (pH 7.0) respectively. As shown in Figure 2A, once the dep-Au nanomaterial was introduced onto electrode surface by electro-deposition, the electrochemical signal of $[Fe(CN)_6]^{3-/4-}$ increased significantly (curve b) due to the good conductivity of dep-Au compared with the bare GCE (curve a). From the Figure 2B, when the double strand DNA A1-A2 was captured onto electrode surface by Au-N bonding, typical

oxidative peaks of MB (-0.3 V) and Fc (0.45 V) was obtained (curve a). Once the HT was introduced into the electrode surface to block the nonspecific site, the electrochemical signals of MB and Fc decreased (curve b). While targets miRNA-155 and miRNA-21, DNA robot and Nt.BbvCI were dropped onto the electrode surface, the corresponding electrochemical signals of MB and Fc (curve c) significantly decreased simultaneously, attributing that targets could trigger the aPLA, further induce the cleaving of Nt.BbvCI. These results confirmed that this electrochemical biosensor could realize simultaneously detection of miRNA-155 and miRNA-21. Moreover, the electrochemical impedance spectroscopy (EIS) characterizations of the modified electrode was performed, and the related results could be seen in the Supporting Information.

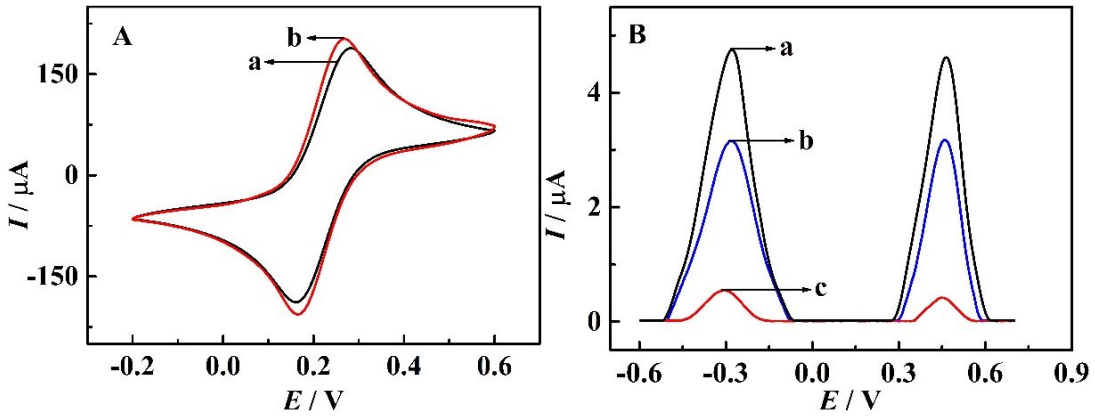

Figure 2. (A) CV responses of different modified electrodes in 2 mL $[Fe(CN)_6]^{3-/4-}$ solution: GCE (a), dep-Au/GCE (b), (B) SWV responses of the different modified electrodes corresponding to the electrochemical signals of MB (-0.3 V) and Fc (0.45 V) for the detection of miRNA-155 and miRNA-21 respectively in 2 mL PBS solution: (a) A1-A2/dep-Au/GCE, (b) HT/A1-A2/ dep-Au/GCE, (c) miRNA-155 + miRNA-21 + DNA robot + Nt.BbvCI/ A1-A2/HT/dep-Au/GCE.

Comparison of Current Response Under Different Conditions. In order to present the multiplexed performance of the proposed biosensor for miRNA-155 and miRNA-21 detection simultaneously, the control experiments under different conditions were carried out. From Figure 3A, when the biosensor incubated without any target miRNAs, it exhibited two typical high signal peaks of MB (-0.30 V) and Fc (0.45 V) at different potential positions respectively. Once the target miRNA-155 (10 pM) was introduced into this biosensor, significant decrease in electrochemical signal of MB was obtained, while the current response corresponding to Fc was still unchanged (Figure 3B), likewise, the introduction of miRNA-21 (10 pM) led to the decreased current response of Fc and the unchanged current response of MB (Figure 3C). The results demonstrated that the proposed biosensor could be employed for the detection of either miRNA-21 or miRNA-155. Significantly, when the biosensor was incubated with miRNA-155 and miRNA-21 simultaneously, obvious decrease in current responses of MB or Fc were observed (Figure 3D), proving that the proposed biosensor could be used to detect multiple miRNAs. Additionally, the comparison of electrochemical signal between the modified electrode in the presence of the nanorobot but without the enzyme and the modified electrode without the nanorobot was performed to further prove the feasibility the proposed biosensor for multiple targets in the presence of DNA robot and enzyme, and the results could be seen from Supporting Information.

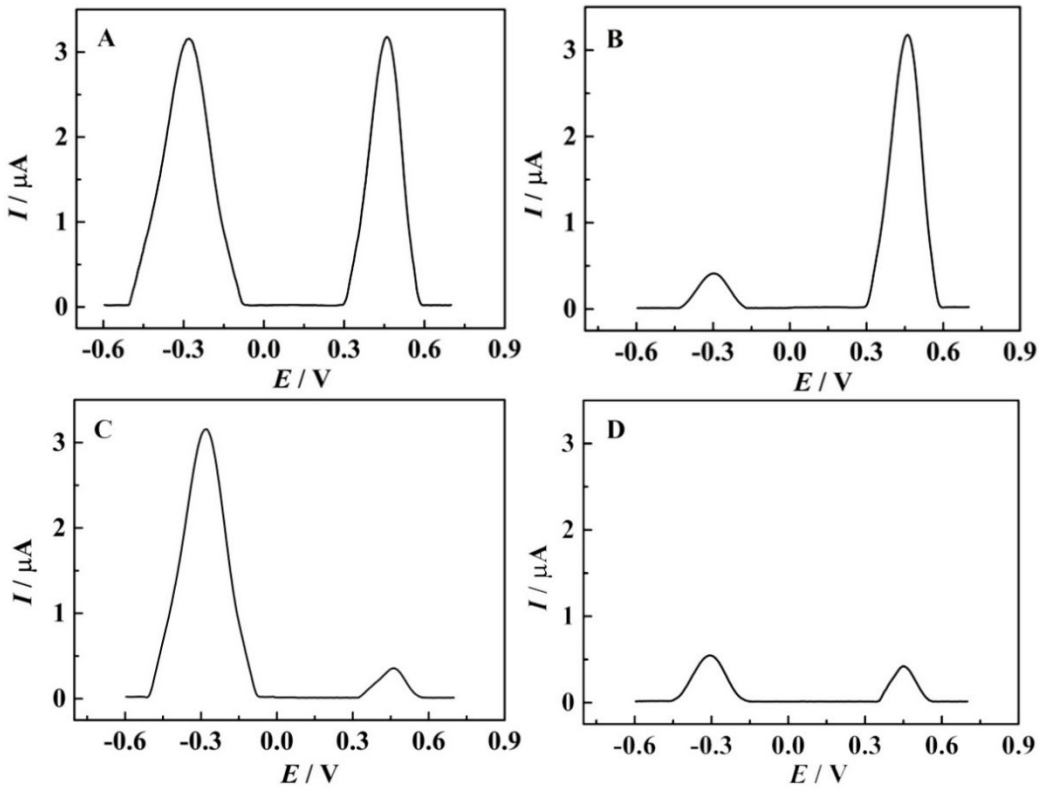

Figure 3. SWV responses of MB (-0.3 V) and Fc (0.45 V) for miRNA-155 and miRNA-21 detection respectively in this electrochemical biosensor: (A) in the absence of miRNA-155 (10 pM) or miRNA-21 (10 pM), in the presence of (B) miRNA-155 (10 pM), (C) miRNA-21 (10 pM), and (D) miRNA-21 (10 pM) and miRNA-155 (10 pM).

Electrochemical Assay of miRNAs Detection. To analyze the detection performance of the biosensor, different concentrations of miRNA-155 and miRNA-21 were measured by SWV under the optimal experimental conditions. As we can see from Figure 4A, increased suppression of the current responses of MB (-0.3 V) and Fc (0.45 V) could be observed with elevated concentration of the target miRNA-155 and miRNA-21 respectively. It was clearly displayed that introducing different concentrations of target miRNAs to this detection system led to obvious decreased in electrochemical signals of Fc and MB. And the calibration plots both in Figure 4B

and 4C displayed well linear relationships for the changes in the SWV signal (ΔI) between different concentration of targets ($\lg c_{miRNAs}$) and blank samples in the dynamic range from 100 aM to 100 pM for miRNA-155 and miRNA-21 respectively. And the regression equation expressed as $\Delta I = 2.273 + 0.302 \lg c_{miRNA\text{-}155}$ and $\Delta I = 2.4 + 0.288 \lg c_{miRNA\text{-}21}$. The corelation coefficients were 0.993, 0.992 and the limit of detections (LOD) were 42.7 aM and 51.1 aM for miRNA-155 and miRNA-21 detection (The detail calculation method of LOD was added in the Supporting Information) respectively. The detection limits of the proposed strategy for multiple miRNAs detection were compared with other reported methods, and displayed wider linear range and more sensitive for miRNAs detection (Table 2).

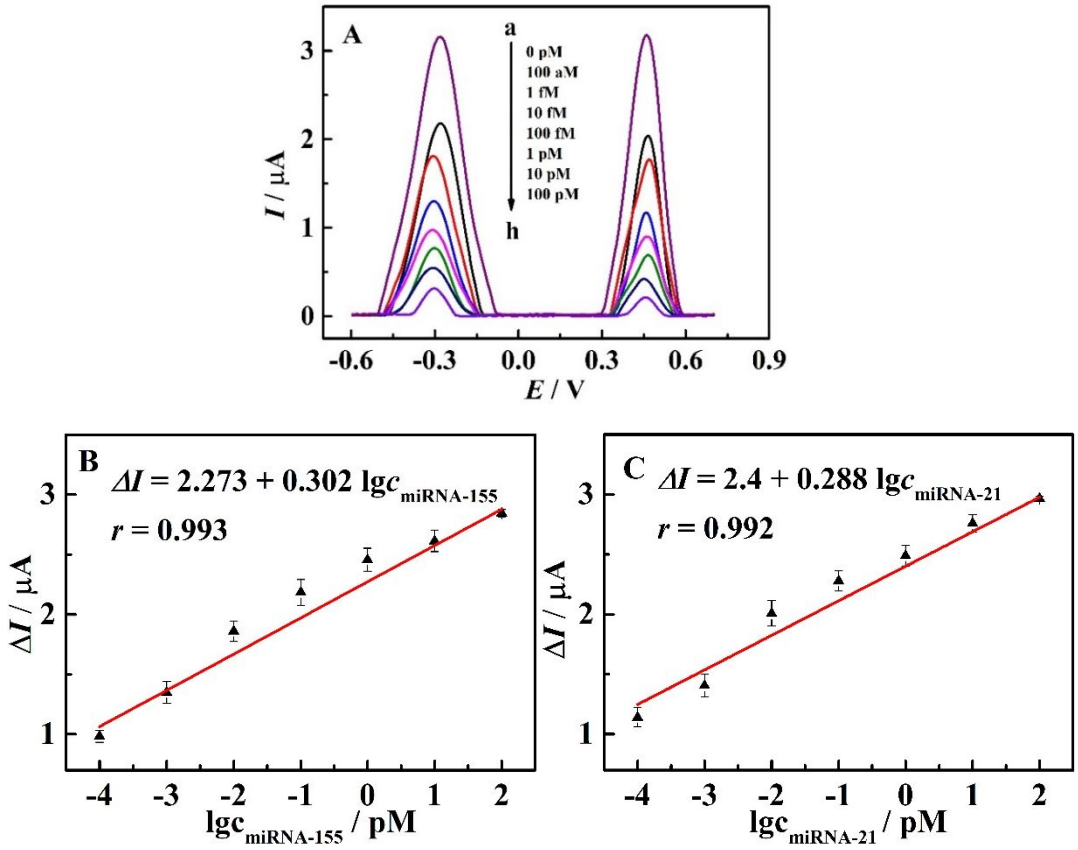

Figure 4. (A) SWV responses of MB (-0.3 V) and Fc (0.45 V) for miRNA-155 and miRNA-21 detection respectively in this electrochemical biosensor at: (a) 0 pM and 0

pM, (b) 100 aM and 100 aM, (c) 1.0 fM and 1.0 fM, (d) 10 fM and 10 fM, (e) 100 fM and 100 fM, (f) 1.0 pM and 1.0 pM, (g) 10 pM and 10 pM, (h) 100 pM and 100 pM. (B) and (C) corresponding to the calibration plots of ΔI vs. $\lg c_{\text{miRNA-155}}$ and $\lg c_{\text{miRNA-21}}$, respectively.

Table 2 Comparison of this strategy with other methods for multiple miRNAs detection.

Analytical method	Target	The limit of detection	References
ECL	miRNA-21/miRNA-155	1.51 fM/1.67 fM	37
FL	miRNA-155/miRNA-210	10 pM/10 pM	38
DPV	miRNA-182/miRNA-381	0.20 fM/0.12 fM	39
SERS	miRNA-21/miRNA-122	2.72 pM/0.24 pM	40
SWV	miRNA-141/miRNA-21	4.2 fM/3.0 fM	41
SWV	miRNA-155/miRNA-21	42.7 aM/51.1 aM	this work

Reproducibility, Selectivity and Stability of the Proposed Biosensor. In order to investigate the reproducibility, six repetitive measurements of 10 pM of miRNA-155 and miRNA-21 respectively achieved the relative standard deviation of 4.83% and 6.21%, confirming the accepted reproducibility of this electrochemical biosensor. While, miRNA-141, miRNA-let7a and miRNA-182-5p were adopted as interfering agents to investigate the selectivity of this biosensor, from Figure 5, we could see that no obvious signal changes of miRNA-144, miRNA-let7a and miRNA-182-5p except that for target miRNAs (10 pM), and the electrochemical signal of the mixture containing miRNA-144 (1.0 nM), miRNA-let7a (1.0 nM), miRNA-182-5p (1.0 nM), miRNA-21(10 pM) and miRNA-155 (10 pM) was similar with that of miRNA-21 (10 pM) and miRNA-155 (10 pM), proving that the present strategy for miRNAs detection possessed good selectivity. Additionally, the prepared fresh electrodes were

used to demonstrate the stability of the designed biosensor, and their electrochemical signals were surveyed after 5d (98.27%/98.58%), 10d (96.16%/97.16%), 15d (95.39%/96.01%), 20d (94.41%/94.73%) and 25d (93.83%/93.35%). These results demonstrated this biosensor owed well stability.

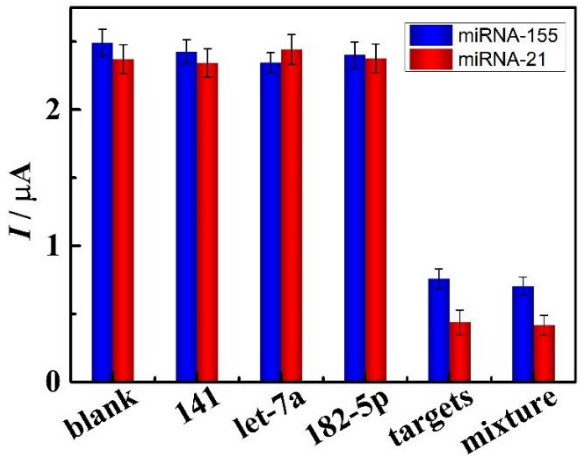

Figure 5. Specificity of the electrochemical biosensor for the blank, miRNA-141(1.0 nM), miRNA-let7a (1.0 nM), miRNA-182-5p (1.0 nM), targets including miRNA-21 (10 pM) and miRNA-155 (10 pM), and the mixture containing miRNA-141 (1.0 nM), miRNA-let7a (1.0 nM), miRNA-182-5p (1.0 nM), miRNA-21 (10 pM) and miRNA-155 (10 pM).

Application. To verify the feasibility of the multiplexed biosensor for miRNAs analysis in real samples, miRNA-155 and miRNA-21 obtained from different cancerous cell lines including MCF-7 (human breast cancer cells) and Hela (cervical cancer cells) were surveyed with this proposed biosensor. As we can see from Figure 6A, bar b showed SWV responses of miRNA-155 from 10^3 Hela and 10^3 MCF-7 respectively, which was lower than that of the blank sample (a). As expected, a gradual decrease in SWV intensities were obtained when the Hela and MCF-7 cells increased to 10^5 (d), suggesting that the miRNA-155 was over-expressed both in Hela

cells and MCF-7 cell. At the same time, the Figure 6B showed that the SWV responses gradually decreased with the MCF-7 cell from 10^3 (b) to 10^5 (d) compared with the blank sample (a), while the SWV responses were hardly any changes with the Hela cell from 10^3 to 10^5. These results demonstrated that the expression level of miRNA-21 in MCF-7 cell was excess, while barely expressed in Hela cell, which were good consistent with previous reports.[42-45] Moreover, the detail process for cell culture and total RNA extraction and the performance analysis of the biosensor for multiple targets in real cell sample could be seen in the Supporting Information.

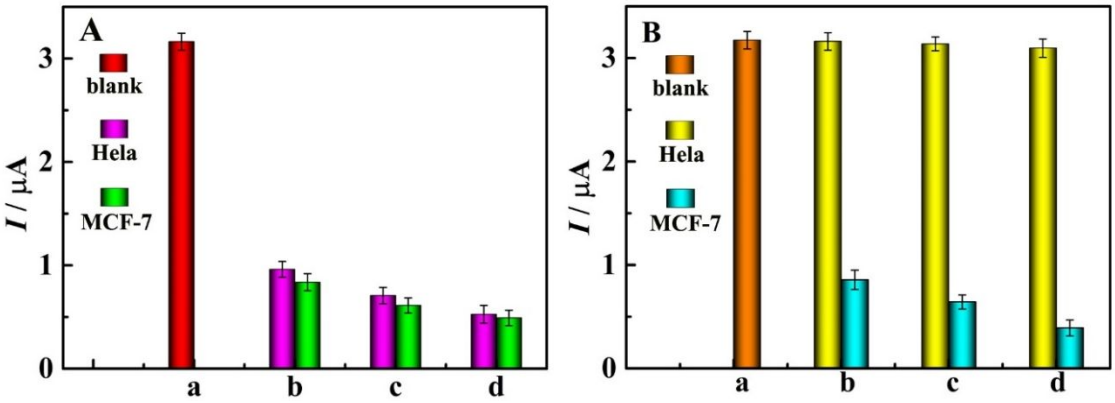

Figure 6. Analysis of miRNA-155 (A) and miRNA-21 (B) from Hela and MCF-7 cells: (a) blank detection without miRNAs; (b) 10^3 cancer cells; (c) 10^4 cancer cells; (d) 10^5 cancer cells.

CONCLUSION

In summary, the present work has designed a classified cargo-discharge DNA robot which was applied in an electrochemical biosensor for the multiple detection of miRNAs by the aPLA-based enzyme cleaving for driving the walking of DNA robot. The proposed electrochemical biosensor showed three attractive features. Firstly, the designed classified cargo-discharge DNA robot possessed high self-assembling and

walking efficiency, which could discharge different cargo (beacons) for increasing the wide application of the proposed biosensor by simply changing the DNA sequences of the feet in DNA robot; Secondly, the aPLA-based enzyme cleaving could not only accelerate the walking speed of DNA robot for reducing the detection time and increasing the detection sensitivity, but also pave a new way for better driving the walking of DNA robot; Thirdly, the introduction of aPLA could enhance the hybridization efficiency of DNA and decrease the unessential DNA sequences, resulting in simplified DNA design and low experiment cost. Above all, the strategy could provide a highly efficient walking platform for various sensors, as well as has potential applications in clinical therapeutics.

ASSOCIATED CONTENT

Supporting Information

The electrochemical impedance spectroscopy characterizations of the modified electrode, the feasibility analysis of the proposed biosensor for multiple targets in the presence of DNA robot and enzyme, the performance analysis of the biosensor for separate detection different target, cell culture and total RNA extraction, the performance analysis of the biosensor for multiple targets in real cell sample, the detection limit calculation of the proposed biosensor for multiple targets detection.

ACKNOWLEDGEMENT

This paper was financially supported by the National Natural Science Foundation of China (21775124, 21675129 and 21575116) and the Fundamental Research Funds for the Central Universities (XDJK2018AA003), China.

REFERENCES

(1) Kay, E. R.; Leigh, D. A. Rise of the molecular machines, *Angew. Chem. Int. Ed.* **2015**, 54,10080-10088.

(2) Angell, C.; Xie, S.; Zhang L.; Chen, Y. DNA nanotechnology for precise control over drug delivery and gene therap, *Small* **2016**, 12, 1117-1132.

(3) Abendroth, J, M.; Bushuyev, O. S.; Weiss, P. S.; Barrett, C. J. *ACS Nano* **2015**, 9, 7746-7768.

Balzani, V.; Credi, A.; Venturi, M. Molecular devices and machines, *Nanotoday* **2007**, 2, 18-25.

(4) Erbas-Cakmak, S.; Leigh, D. A.; McTernan, C. T.; Nussbaumer, A. L. Artificial molecular machines, *Chem. Rev.* **2015**, 115, 10081-10206.

(5) Cha, T. G.; Pan, J.; Chen, H.R.; Salgado, J.; Li, X.; Mao, C. D.; Choi, J. H. A synthetic DNA motor that transports nanoparticles along carbon nanotubes, *Nat. Nanotech.* **2014**, 9, 39-43.

(6) Kay, E. R.; Leigh, D. A.; Zerbetto, F. Molecular highways–navigating collisions of DNA motor proteins, *Angew. Chem. Int. Ed.* **2007**, 46, 72-191.

(7) Dixit, R.; Ross, J. L.; Goldman, Y. E.; Holzbaur, E. L. F. Differential regulation of dynein and kinesin motor proteins by tau, *Science* **2008**, 319, 1086-1089.

(8) Vale, R. D.; Milligan, R. A. The way things move: looking under the hood of molecular motor proteins, *Science* **2000**, 288, 88-95.

(9) Chuang, C. J.; Li, W. S.; Lai, C. C.; Liu, Y. H.; Peng, S. M.; Chao, I.; Chiu, S. H. A molecular cage-based [2] rotaxane that behaves as a molecular muscle, *Org. Lett.* **2009**, 11, 385-388.

(10) Takezawa, Y.; Shionoya, M. Metal-mediated DNA base pairing: alternatives to hydrogen-bonded Watson-Crick base pairs, *Acc. Chem. Res.* **2012**, 45, 2066-2076.

(11) Gu, H. Z.; Chao, J.; Xiao, S. J.; Seeman, N. C. A proximity-based programmable DNA

nanoscale assembly line, *Nature* **2010**, 465, 202-205.

(12) Wickham, S. F. J.; Bath, J.; Katsuda, Y.; Endo, M.; Hidaka, K.; Sugiyama, H.; Turberfield, A. J. A DNA-based molecular motor that can navigate a network of tracks, *Nat. Nanotech*. **2012**, 7, 169-173.

(13) Chen, Y. J.; Groves, B.; Muscat, R. A.; Seelig G. DNA nanotechnology from the test tube to the cell, *Nat. Nanotechnol.* **2015**, 10, 748-760.

(14) Zhang, F.; Nangreave, J.; Liu Y.; Yan, H. Structural DNA nanotechnology: state of the art and future perspective, *J. Am. Chem. Soc.*, **2014**, 136, 11198-11211.

(15) Tan, S. J.; Campolongo, M. J.; Luo, D.; Cheng, W. L. Building plasmonic nanostructures with DNA, *Nat. Nanotech.* **2011**, 6, 268-276.

(16) Douglas, S. M.; Dietz, H.; Liedl, T.; Högberg, B.; Graf, F.; Shih, W. M. Self-assembly of DNA into nanoscale three-dimensional shapes, *Nature* **2009**, 459, 414-418.

(17) Li, J. M.; Johnson-Buck, A.; Yang, Y. R.; Shih, William, M.; Yan, H.; Walte, N. G. Exploring the speed limit of toehold exchange with a cartwheeling DNA acrobat, *Nature Nanotechnology* **2018**,13, 723-729.

(18) Jung, C.; Allen, P. B.; Ellington, A. D. A stochastic DNA walker that traverses a microparticle surface, *Nat. Nanotech.* **2016**, 11, 157-163.

(19) Thubagere, A. J.; Li, W.; Johnson, R. F.; Chen, Z. B.; Doroudi, S. Y.; Lee, Y. L.; Izatt, G.; Wittman, S.; Srinivas, N.; Woods, D.; Winfree, E.; Qian, L. L. A cargo-sorting DNA robot, *Science* **2017**, 357, 1-9.

(20) Hu, Q. Q; Li, H.; Wang, L. H.; Gu, H. Z.; Fan, C. H. DNA nanotechnology-enabled drug delivery systems, *Chem. Rev.* **2018**, DOI: 10.1021/acs.chemrev.7b00663.

(21) Zeng, S.; Liu, D.; Li, C.Y.; Yu, F.; Fan, L.; Lei, C. Y.; Huang, Y.; Nie, Z.; Yao S. Z., Cell-surface-anchored ratiometric DNA tweezer for real-time monitoring of extracellular and apoplastic pH, *Anal. Chem.*, **2018**, 90, 13459-13466.

(22) Fu, T.; Lyu, Y. F.; Liu, Hui.; Peng, R. Z.; Zhang, X. B.; Ye, M.; Tan, W. H. DNA-based dynamic reaction networks, *Trends Biochem. Sci.* **2018**, 43, 547-560.

(23) Yehl, K.; Mugler, A.; Vivek, S.; Liu, Y.; Zhang, Y.; Fan, M. Z.; Weeks, E. R.; Salaita, K. High-speed DNA-based rolling motors powered by RNase H, *Nat. Nanotech.* **2016**, 11, 184-190.

(24) Balzani, V.; Credi, A.; Venturi, M. Light powered molecular machines, *Chem. Soc. Rev.* **2009**, 38, 1542-1550.

(25) Lohmann, F.; Ackermann, D.; Famulok, M. Reversible light switch for macrocycle mobility in a DNA rotaxane, *J. Am. Chem. Soc.* **2012**, 134, 11884-11887.

(26) Green, S. J.; Bath, J.; Turberfield, A. J. Coordinated chemomechanical cycles: a mechanism for autonomous molecular motion, *Phys. Rev. Lett.* **2008**, 101, 238101-1-238101-4.

(27) Yin, P.; Yan, H.; Daniell, X. G.; Turberfield, A. J.; Reif, J. H. *Angew. Chem.* **2004**, 116, 5014-5019.

(28) He, Y.; Liu, D. R. Autonomous multistep organic synthesis in a single isothermal solution mediated by a DNA walker, *Nat. Nanotech.* **2010**, 5, 778-782.

(29) You, M. X.; Chen, Y.; Zhang, X. B.; Liu, H. P.; Wang, R. W.; Wang, K. L.; Williams, K. R.; Tan, W. H. An autonomous and controllable light-driven DNA walking device, *Angew. Chem. Int. Ed.* **2012**, 51, 2457-2460.

(30) Shin, J. S.; Pierce, N. A. A synthetic DNA walker for molecular transport, *J. Am. Chem. Soc.* **2004**, 126, 10834-10835.

(31) Yang, X. L.; Tang, Y. N.; Mason, S. D.; Chen, J. B.; Li, F. Enzyme-powered three-dimensional DNA nanomachine for DNA walking, payload release, and biosensing, *ACS Nano* **2016**, 10, 2324-2330.

(32) Li, Y. Y.; Wang, G. A.; Mason, S. D.; Yang, X. L.; Yu, Z. C.; Tang, Y. N.; Li, F. Simulation-guided engineering of an enzyme-powered three dimensional DNA nanomachine for discriminating single nucleotide variants, *Chem. Sci.* **2018**, 9, 6434-6439.

(33) Li, F.; Zhang, H. Q.; Wang, Z. X.; Li, X. K.; Li, X. F.; Le, X. C. Dynamic DNA assemblies mediated by binding-induced DNA strand displacement, *J. Am. Chem. Soc.* **2013**, 135, 2443-2446.

(34) Fredriksson, S.; Gullberg, M.; Jarvius, J.; Olsson, C.; Pietras, K.; Gústafsdóttir, S. M.; Östman, A.; Landegren, U. Protein detection using proximity-dependent DNA ligation assays, *Nat. biotech.* **2002**, 20, 473-477.

(35) Liu, S. F.; Fang, L.; Wang, Y. Q.; Wang, L. Universal dynamic DNA assembly-programmed surface hybridization effect for single-step, reusable, and amplified electrochemical nucleic acid biosensing, *Anal. Chem.* **2017**, 89, 3108-3115.

(36) Zhang, X. L.; Yang, Z. H.; Chang, Y. Y.; Qing, M.; Yuan, R.; Chai, Y. Q. Novel 2D-DNA-nanoprobe-mediated rnzyme-free-target-recycling amplification for the ultrasensitive electrochemical detection of microRNA, *Anal. Chem.* **2018**, 90, 9538-9544.

(37) Peng, L.; Zhang, P.; Chai, Y.; Yuan, R. Bi-directional DNA walking machine and its application in an enzyme-free electrochemiluminescence biosensor for sensitive detection of microRNAs, *Anal. Chem.* **2017**, 89, 5036-5042.

(38) Wang, C.; Zhang, H.; Zeng, D.; Sun, W.; Zhang, H.; Aldalbahi, A.; Wang, Y.; San, L.; Fan, C.; Zuo, X.; Mi, X. Elaborately designed diblock nanoprobes for simultaneous multicolor

detection of microRNAs, *Nanoscale* **2015**, 7, 15822-15829.

(39) Wang, J. R.; Lu, Z. X.; Tang, H. L.; Wu, L.; Wang, Z. X.; Wu, M. H.; Yi, X. Y.; Wang, J. X. Multiplexed electrochemical detection of miRNAs from sera of glioma patients at different stages via the novel conjugates of conducting magnetic microbeads and diblock oligonucleotide-modified gold nanoparticles, *Anal. Chem.* **2017**, 89, 10834-10840.

(40) Zhou, W.; Tian, Y. F.; Yin, B. C.; Ye, B. C. Simultaneous surface-enhanced Raman spectroscopy detection of multiplexed microRNA biomarkers, *Anal. Chem.* **2017**, 89, 6120-6128.

(41) Yang, C. Y.; Dou, B. T.; Shi, K.; Chai, Y. Q.; Xiang, Y.; Yuan, R. *Anal. Chem.* **2014**, 86, 11913-11918.

(42) Yu, S.; Wang, Y. Y.; Jiang, L. P.; Bi, S.; Zhu J. J. Cascade amplification-mediated in situ hot-spot assembly for microRNA detection and molecular logic gate operations, *Anal. Chem.* **2018**, 90, 4544-4551.

(43) Lu, S. S.; Wang, S.; Zhao, J. H.; Sun, J.; Yang, X. R. Fluorescence light-up biosensor for MicroRNA based on the distance-dependent Photoinduced electron transfer, *Anal. Chem.* **2017**, 89, 8429-8436.

(44) Yue, S. Z.; Song, X. Y.; Song, W. L.; Bi, S. An enzyme-free molecular catalytic device: dynamically self-assembled DNA dendrimers for in situ imaging of microRNAs in live cells, *Chem. Sci.* **2019**, 10, 1651-1658.

(45) Lu, L. P.; Wang, J. X.; Miao, W. J.; Wang, X. Y.; Guo, G. S. Electrogenerated chemiluminescence biosensor with a tripod probe for the highly sensitive detection of microRNA, *Anal. Chem.* **2019**, 91, 1452-1459.

For TOC only